Tuned Optical Receivers for Microwave Subcarrier Multiplexed Lightwave Systems

KAMAL E. ALAMEH, STUDENT MEMBER, IEEE, AND ROBERT A. MINASIAN, MEMBER, IEEE

Abstract—An analysis of tuned optical receiver noise performance for microwave subcarrier multiplexed lightwave systems is presented. The effect of correlation between the gate and the drain HEMT noise sources is included, and the design of tuning networks to obtain partial noise cancellation is investigated. An optimization algorithm is used to determine the tuning element values for minimizing noise. Improvements in noise of 16 dB for a 60 video channel SCM system, and 12 dB for a 120 channel system are demonstrated, allowing a significant increase in passive optical network distribution capacity, and design results for tuned front-end receivers encompassing the effects of p-i-n, HEMT and SCM band parameters are presented.

I. Introduction

RECENT advances in high-speed optoelectronic components have made microwave subcarrier multiplexing (SCM) an attractive technique for multichannel lightwave distribution networks. Notable system results have been demonstrated involving 120 channel video transmission [1], 2 and 4 Gb/s data links [2], [3], and wide-band digital multiuser networks [4]. These lightwave systems combine the advantages of multi-GHz data throughputs using established microwave techniques with the versatile analog and digital modulation formats [5], for evolution with emerging network requirements.

In order to achieve large point-to-multipoint distribution capacity, a high power budget is required for SCM systems. The use of optical amplifiers to increase the power budget has received considerable attention. Both in-line traveling wave laser amplifiers preceding the optical splitter [6], [7] and optical preamplifiers at the receiver [8] have been reported. However, a distribution topology based on the passive optical network (PON) concept [9] provides more attractive features regarding installation simplicity, reliability, and cost. Improvements in modulation and output of laser transmitters for SCM PON systems have been presented recently [10]. This paper presents complementary studies for increasing the power budget and distribution capacity through enhanced receiver sensitivity.

Tuning of optical receiver front ends has been shown to be an effective technique for reducing high-frequency receiver noise. This has been demonstrated both theoretically and experimentally for wide-band direct detection systems [11], coherent systems [12], [13], and SCM systems [14]. The object of this paper is to present a detailed noise analysis for the design of tuned p-i-n HEMT optical SCM receivers. A new contribution is provided by the analysis, through the incorporation of the correlation effects between the gate and drain noise sources of the FET [15], [16]. Previous analyses [11]–[14] have relied on the Ogawa noise factor, Γ [17], to account for noise correlation in FET's, even though the concept of a constant noise factor breaks down for tuned front-end amplifiers. The inclusion of detailed correlation effects leads to improved accuracy for design and is particularly relevant to HEMT devices which have high correlation coefficients [15] and which consequently afford the potential of partial noise cancellation through appropriate tuning network design. A general optimization of the tuning network is carried out to minimize the input equivalent noise arising from the FET noise, Johnson resistor noise in the p-i-n and HEMT, and shot noise. The results indicate substantial improvements in receiver sensitivity for 60 channel (2.7–5.2 GHz) and 120 channel (2.7–7.7 GHz) video systems.

The noise analysis of tuned receivers including correlation effects is presented in Section II. Section III presents design information for tuned receivers and shows noise characteristics. Finally, results are given for a 60 channel microwave SCM system which show how the enhanced receiver sensitivity allows increased distribution capability.

II. Tuned Receiver Noise Analysis

A. Device Noise Models

The noise equivalent circuit for the HEMT is shown in Fig. 1(a). The intrinsic behavior of the transistor is described [15] by the drain noise, gate noise, and correlation coefficient, given by

$$\overline{i_{nd}^2} = 4kTPg_m\Delta f \tag{1}$$

$$\overline{i_{ng}^2} = 4kTR\frac{(\omega C_{GS})^2}{g_m}\Delta f \tag{2}$$

$$\overline{i_{ng}^* i_{nd}} = jC_{\text{cor}}\sqrt{PR}\,4kT(\omega C_{GS})\,\Delta f. \tag{3}$$

Manuscript received July 18, 1989, revised November 27, 1989. This work was supported by the Australian Research Council.

The authors were with the Department of Electrical and Electronic Engineering, University of Melbourne, Parkville, 3052, Australia. They are now with the School of Electrical Engineering, University of Sydney, Sydney, NSW, 2006, Australia.

IEEE Log Number 8934032.

0018-9480/90/0500-0546$01.00

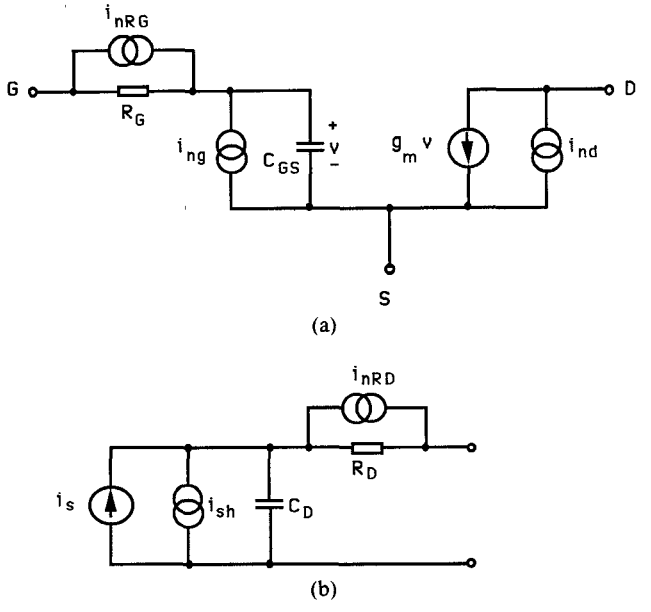

Fig. 1. Device noise models. (a) HEMT noise equivalent circuit: $g_m = 55$ mS, $C_{GS} = 0.25$ pF, $R_G = 1\ \Omega$, $P = 1$, $R = 0.5$, $C_{cor} = 0.9$ (b) p-i-n equivalent circuit: $C_D = 0.12$ pF, $R_D = 10\ \Omega$.

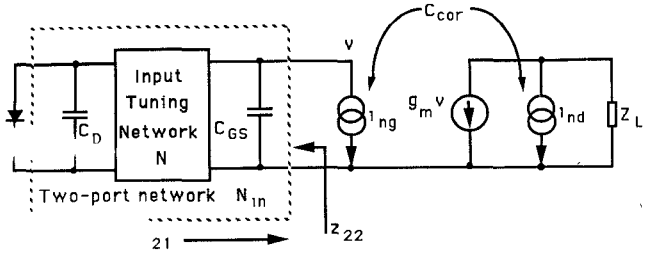

Fig. 2. General tuned p-i-n FET front-end circuit.

For a $0.5 \times 200\ \mu m^2$ gate HEMT [18], the noise coefficient values $P = 1$, $R = 0.5$, and $C_{cor} = 0.9$ have been shown to give good agreement with measured noise figure data [15]. The gate resistor noise source is given by

$$\overline{i_{nR_G}^2} = \frac{4kT}{R_G}\Delta f. \tag{4}$$

Fig. 1(b) shows the equivalent circuit for the p-i-n diode. The shot noise current source is described by

$$\overline{i_{sh}^2} = 2qI_{dc}\Delta f \tag{5}$$

where I_{dc} is the average detected photocurrent, and the series resistor thermal noise is given by

$$\overline{i_{nR_D}^2} = \frac{4kT}{R_D}\Delta f. \tag{6}$$

B. General Tuned Network Requirements

We consider a general input tuning network interposed between the photodiode and the FET, in order to establish the required circuit characteristics for minimizing the effects of FET noise. This is shown by the network N in Fig. 2, where C_D represents the photodiode capacitance, C_{GS} is the FET gate capacitance, Z_L is the amplifier load impedance, and i_{ng}, and i_{nd} are the correlated gate and drain noise sources of the FET. The complete input network comprising N, C_D, and C_{GS} is defined as a two-port network N_{in} described by z parameters. The equivalent input noise current is given by

$$\frac{\overline{i_{in}^2}}{\Delta f} = \frac{4kT}{g_m}\frac{\Gamma(z_{22})}{|z_{21}|^2} \tag{7}$$

where

$$\Gamma(z_{22}) = P + (|z_{22}|\omega C_{GS})^2 R - 2C_{cor}\sqrt{PR}\,(\omega C_{GS}\,\mathrm{Im}[z_{22}]) \tag{8}$$

is identified as the FET noise factor [17]. This is an extension of the Ogawa analysis [17], and reduces to the same result when the front end is untuned with $z_{22} = 1/[j\omega(C_D + C_{GS})]$.

For the untuned case, (8) shows that the noise factor is constant and that the correlation term is additive so that Γ is increased. For the tuned case Γ in general becomes frequency dependent. Equations (7) and (8) give the conditions required to minimize the input noise current $\overline{i_{in}^2}$. In order to reduce the noise factor, it is required that $\mathrm{Im}[z_{22}] > 0$, so that the correlation C_{cor} term subtracts in (8); i.e., the reactance seen by the gate noise generator i_{ng} should be inductive. More particularly, the optimum value is given by

$$\mathrm{Im}[z_{22,opt}] = \frac{1}{\omega C_{GS}} C_{cor}\sqrt{\frac{P}{R}} \tag{9}$$

which from (8) results in

$$\Gamma_{min} = P(1 - C_{cor}^2). \tag{10}$$

Equation (10) shows that Γ can be reduced significantly due to cancellation of noise through correlation if the input network can present an inductive reactance decreasing with frequency according to (9). The cancellation effect is particularly relevant for HEMT's where the factor $(1 - C_{cor}^2)$ can be quite small. The second requirement in (7) for minimizing the noise is that $|z_{21}|$ be maximized. This implies that the network should have a resonance within the passband for maximizing the transfer of input signal to the gate.

The simultaneous requirements on the network z_{22} and z_{21} parameters for minimizing noise can best be achieved by optimization of the elements in network N. A specific tuning circuit is considered in the next section.

C. Tuned Front-End Analysis

The circuit configuration of a tuned p-i-n HEMT front end is shown in Fig. 3(a). A T-topology broad-band tuning network is shown; however, depending on the detailed specification of L_1, L_2, and L_3, this also incorporates series, parallel, L, and Π networks. The circuit includes an FET source inductance L_s which is effective in making the frequency response more uniform [14]. Fig. 3(b) gives the equivalent circuit for the receiver front end showing the

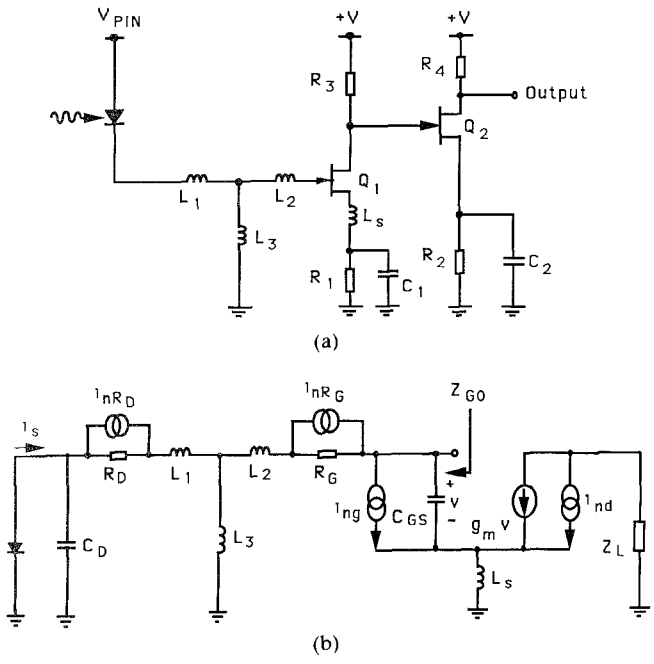

Fig. 3. Tuned p-i-n FET front end (a) Circuit configuration (b) Equivalent circuit including noise sources.

various noise sources. Defining

$$Z_D = 1/j\omega C_D \tag{11}$$

$$Z_1 = R_D + j\omega L_1 \tag{12}$$

$$Z_2 = R_G + j\omega L_2 \tag{13}$$

$$Z_3 = j\omega L_3 \tag{14}$$

$$Z_{GS} = 1/j\omega C_{GS} \tag{15}$$

$$Z_s = j\omega L_s \tag{16}$$

and

$$Z_2' = Z_2 + Z_3' \tag{17}$$

$$Z_3' = Z_3 \| (Z_D + Z_1) \tag{18}$$

the transfer function of the front end is given by

$$Z_{21} = \frac{v}{i_s} = \frac{Z_D Z_3' Z_{GS}}{(Z_D + Z_1)[(1 + g_m Z_s) Z_{GS} + Z_2' + Z_s]}. \tag{19}$$

The equivalent input noise current component due to the FET noise sources is

$$\frac{\overline{i_{\text{inFET}}^2}}{\Delta f} = \frac{4kT}{g_m} \frac{1}{|Z_{21}/A|^2} \left\{ P + R|Z_{G0}|^2 (\omega C_{GS})^2 - 2C_{\text{cor}}\sqrt{PR}\,(\omega C_{GS}\,\text{Im}[Z_{G0}]) \right\} \tag{20}$$

where

$$Z_{G0} = Z_{GS} \| (Z_2' + Z_s) \tag{21}$$

$$A = \frac{Z_{GS} + Z_2' + Z_s}{Z_{GS} + Z_2' + Z_s(1 + g_m Z_{GS})}. \tag{22}$$

These expressions describe the noise characteristics with L_s included; otherwise they are similar in form to (7) and (8). Z_{G0} can be identified as the impedance seen by the gate noise generator i_{ng} with g_m set to zero, and this impedance has a role in determining the noise factor analogous to z_{22}. The term $|Z_{21}/A|$ accounts for the modification in the transimpedance transfer function due to the presence of L_s.

Additional components in the equivalent input noise current arise from

$$\frac{\overline{i_{\text{in}\,R_D}^2}}{\Delta f} = 4kT\frac{R_D}{|Z_D|^2} \tag{23}$$

and from R_G:

$$\frac{\overline{i_{\text{in}\,R_G}^2}}{\Delta f} = 4kTR_G \left| \frac{Z_D + Z_1}{Z_D + Z_3'} \right|^2. \tag{24}$$

The total circuit noise current referred to the input is given by

$$\overline{i_{\text{in}}^2} = \overline{i_{\text{inFET}}^2} + \overline{i_{\text{in}\,R_D}^2} + \overline{i_{\text{in}\,R_G}^2} \tag{25}$$

which is minimized by appropriate tuning network design.

III. Results

The optical p-i-n HEMT front end shown in Fig. 3 was analyzed using the device models given in Fig. 1. A computer optimization procedure was employed to obtain the values of L_1, L_2, and L_3 in the tuning network which minimizes the peak of the input noise current $\overline{i_{\text{in}}^2}$ (described by (20)–(25)) within an operating bandwidth of interest. This optimization was general for minimizing the input noise, without constraints regarding the relation between the resonance frequencies of the tuning network [12]. The results gave the tuned front-end design for maximizing the signal-to-noise ratio in a given SCM bandwidth. The microwave frequency bands considered corresponded to previously reported SCM systems and were (i) 2.7 to 5.2 GHz for 60 channel video transmission [10], [19] and (ii) 2.7 to 7.7 GHz for 120 channel video transmission [1].

The input noise current spectral density resulting from the optimum tuning network $L_1 = 10.2$ nH, $L_2 = 0.7$ nH, and $L_3 = 3.8$ nH (with $L_s = 0.4$ nH) for the 60 channel system is shown in Fig. 4(a). The peak noise current is $4 \cdot 10^{-24}$ A^2/Hz. The tuned design achieves an improvement in noise power across the octave band of more than 9 dB relative to the untuned front end and more than 16 dB relative to the 3 dB noise figure amplifier employed in [10] and [19]. This represents a significant receiver sensitivity improvement with consequent power budget and system performance enhancements. Fig. 4(a) also gives the relative contribution of the various noise sources and shows that the FET noise and R_D noise are the main components. The corresponding noise spectrum for the 120 channel system with an optimum tuning network $L_1 = 5.0$ nH, $L_2 = 0.0$ nH, and $L_3 = 3.6$ nH ($L_s = 0.4$ nH) is shown in Fig. 4(b). The peak noise current is $1.15 \cdot 10^{-23}$ A^2/Hz. The tuned design achieves an improvement in noise power of 12 dB across the band relative to the 3 dB noise figure amplifier employed in [1].

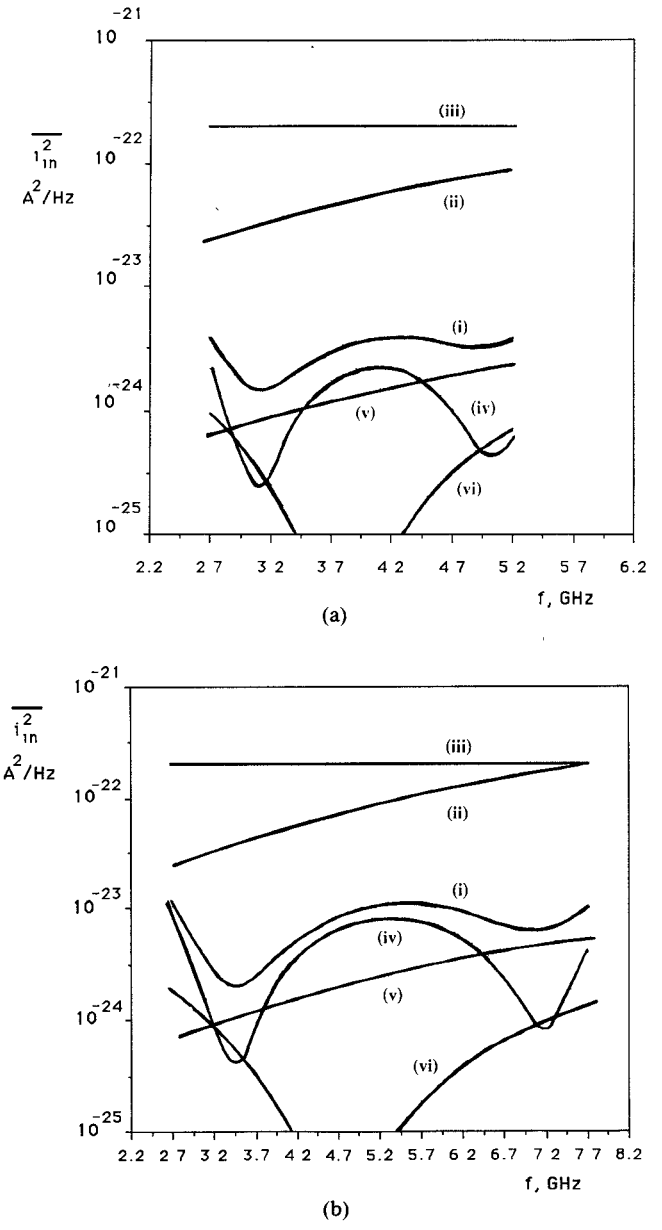

Fig. 4. Input noise channel spectral density. (a) 60 channel, 2.7–5.2 GHz band: (*i*) tuned front-end, (*ii*) untuned, (*iii*) 3 dB noise figure amplifier, (*iv*) FET noise, (*v*) R_D noise, (*vi*) R_G noise. (b) 120 channel, 2.7–7.7 GHz band: (*i*) tuned front-end, (*ii*) untuned, (*iii*) 3 dB noise figure amplifier, (*iv*) FET noise, (*v*) R_D noise, (*vi*) R_G noise.

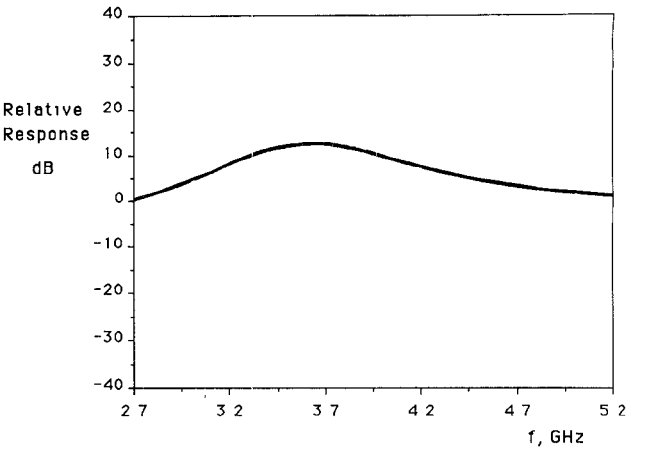

Fig. 5. Front-end signal frequency response.

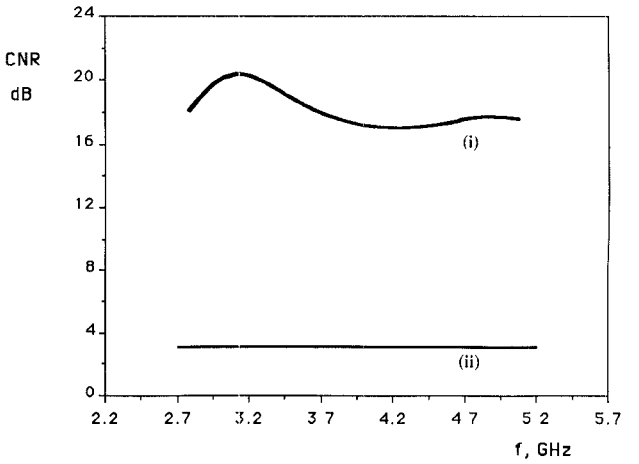

Fig. 6. Carrier-to-noise ratio in a 30 MHz bandwidth subcarrier channel versus center frequency of channel for 60 channel front end: (*i*) tuned front end; (*ii*) 3 dB noise figure amplifier.

The signal frequency response for the front end is displayed in Fig. 5. The FET source inductance L_s is effective in making the frequency response more uniform, without degrading noise performance.

The carrier-to-noise ratio performance in a 30 MHz bandwidth subcarrier video channel for the 60 channel tuned front end design is shown in Fig. 6. This has been obtained for a detected photocurrent of $I_{dc}=1.5\ \mu$A, with a modulation index identical to [10] of $m=7.7\%$. The dominant noise component that determines the CNR for these conditions is the front-end circuit noise, which has a maximum value of $4.0\cdot10^{-24}$ A²/Hz, as shown in Fig. 4(a). Other noise components are the shot noise at $0.48\cdot10^{-24}$ A²/Hz, RIN noise at $0.07\cdot10^{-24}$ A²/Hz (for a laser RIN of -135 dB/Hz), and third-order intermodulation product (IMP) noise at $0.08\cdot10^{-24}$ A²/Hz. The IMP noise has been estimated from [19], [20]

$$\overline{i_{n\mathrm{IM}_3}^2}=\frac{1}{2}(mI_{dc})^2(m^2\mathrm{IM}_3)^2\left[\frac{r_{DN21}}{4}+r_{DN111}\right]\frac{1}{B} \quad (26)$$

where $\mathrm{IM}_3\leqslant 0.1$, as in [19], B is the channel bandwidth, and r_{DN21} and r_{DN111} are the numbers of IM products of type $2f_1-f_2$ and type $f_1\pm f_2\pm f_3$, respectively, falling in the worst channel at the center of the transmission band [20]. Fig. 6 shows that a broadcast-quality CNR of 16.5 dB is obtained for the tuned front end at a detected photocurrent of $I_{dc}=1.5\ \mu$A. This represents a 7.3 dB improvement in optical sensitivity compared to the receiver employed in [10].

Additional data for the 60 channel tuned front-end design are presented in Figs. 7 to 9. The optimum tuning inductance and resulting noise characteristics for different p-i-n diode capacitance values are given in Fig. 7. Fig. 8 shows how the optimum tuning inductances and noise depend on the HEMT g_m and C_{GS} parameters. It is evident that the inductance values in all these cases range to about 10 nH, and are all realizable components. Finally,

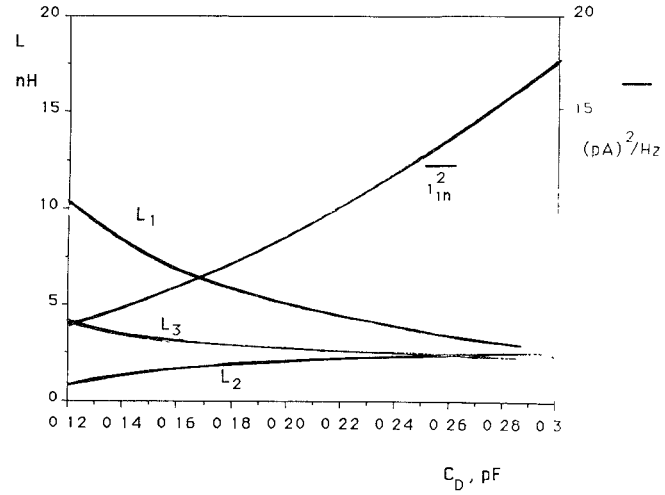

Fig. 7. Optimum tuning inductances and resulting noise characteristics versus p-i-n diode capacitance.

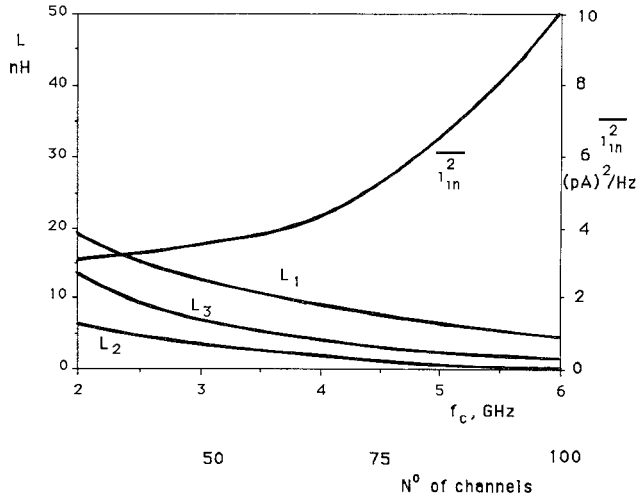

Fig. 9. Optimum tuning inductances and noise characteristics as a function of the number of 40 MHz video channels for transmission and corresponding SCM center frequency.

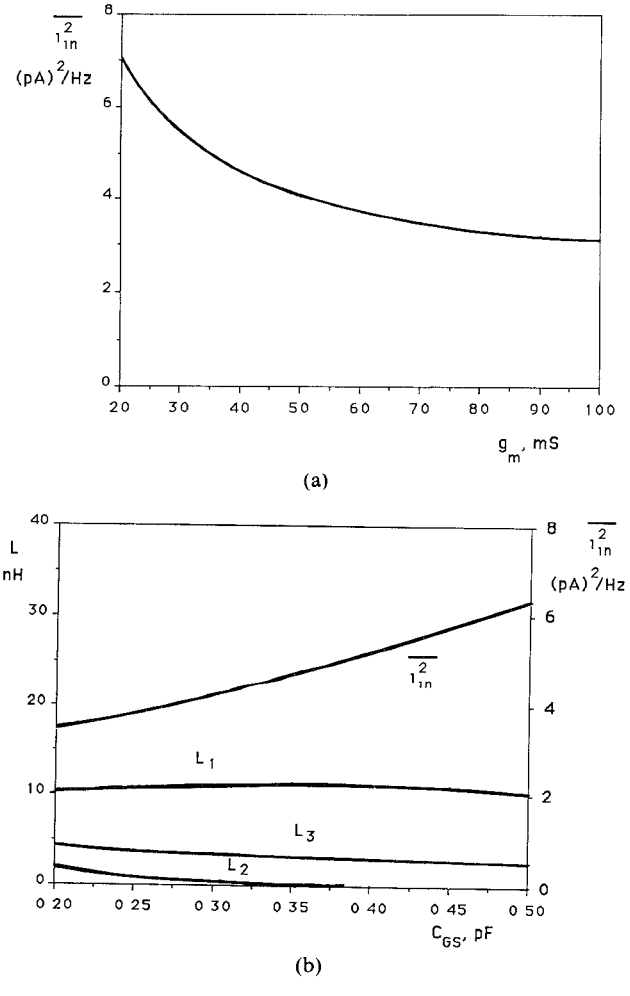

Fig. 8. Effect of HEMT parameters (a) Dependence of input noise current on transconductance g_m. (b) Dependence of tuning inductances and noise current on gate capacitance C_{GS}.

Fig. 9 gives design information showing the optimum inductances and noise for other octave bandwidth SCM systems transmitting different numbers of video channels.

To put these results into context, the sensitivity of the tuned front end for the 60 channel video system and the corresponding system power budget have been calculated to determine the PON distribution capability. For a laser transmitter modulation index of $m = 7.7\%$/channel, as in [10], the sensitivity in terms of the received optical power for a CNR of 16.5 dB (corresponding to a weighted SNR of around 56 dB) is -28 dBm, with a p-i-n responsivity of 1 A/W. This provides a power budget of 31 dB, for a laser launch power of $+3$ dBm, as in [10]. Allowing a 5 dB link loss and 5 dB margin [10] results in 21 dB being available for passive optical splitting. Hence a 64 way splitter having an 18 dB theoretical loss can be used, with a margin for practical losses. This represents a fourfold increase in distribution capacity over a PON compared to the system in [10], which employs a 3 dB noise figure amplifier, and is a direct consequence of the improved tuned receiver sensitivity performance.

IV. Conclusion

An analysis of tuned optical receivers for microwave subcarrier multiplexed lightwave systems has been presented. The analysis has included the detailed effects of correlation between the gate and drain FET noise sources, which has not been previously considered. Results have shown that the FET noise factor is in general frequency dependent for tuned front ends and that, through appropriate tuning network design, partial noise cancellation can be obtained to improve noise performance, particularly for HEMT devices which have high correlation coefficients. Input tuning network circuit requirements have been established, and a detailed analysis was given for a specific tuning configuration. A general optimization was carried out for the design of tuned front ends with minimum input equivalent noise, and design information showing noise

characteristics and effects of p-i-n, HEMT, and SCM band parameters was presented. The tuned front-end designs resulted in substantial noise improvements (16 dB for a 60 video channel SCM system and 12 dB for a 120 channel system) relative to previously reported performances with 3 dB noise figure microwave amplifiers. The corresponding receiver sensitivity improvement of 7.3 dB for the 60 channel system made possible a fourfold increase in distribution capacity over a passive optical network, to 64 terminals. Results have shown that the development of low-noise tuned front ends is an effective means of increasing the power budget for multichannel transmission. This should find application in the design of high-sensitivity receivers for multiaccess, microwave multiplexed lightwave systems.

REFERENCES

[1] R. Olshansky, V. Lanzisera, and P. Hill, "Design and performance of wideband subcarrier multiplexed lightwave systems," in *Proc. European Conf. Opt. Commun.*, 1988, pp. 143–146.

[2] P. Hill and R. Olshansky, "Twenty channel FSK subcarrier multiplexed optical communication system for video distribution," *Electron Lett.*, vol. 24, pp. 892–894, 1988.

[3] K. Runge, W. Way, and N. Cheung, "4 GB/s subcarrier multiplexed transmission over 30 km using microwave QPSK modulation," in *Proc. Opt. Fibre Commun. Conf.*, 1989, pp. PD18-1 to PD18-4.

[4] T. Darcie *et al.*, "Wide-band lightwave distribution system using subcarrier multiplexing," *J. Lightwave Technol.*, vol. 7, pp. 997–1004, 1989.

[5] R. Olshansky, V. Lanzisera, and P. Hill, "Simultaneous transmission of 100 Mbit/s at baseband and 60 FM video channels for a wideband optical communication network," *Electron. Lett.*, vol. 24, pp. 1234–1235, 1988.

[6] W. Way *et al.*, "90 channel FM video transmission to 2048 terminals using two inline traveling wave laser amplifiers in a 1300 nm subcarrier multiplexed optical system," in *Proc. European Conf. Opt. Commun.*, 1988, pp. 37–40.

[7] R. Olshansky and E. Eichen, "Microwave-multiplexed wideband lightwave systems using optical amplifiers for subcarrier distribution," *Electron. Lett.*, vol. 24, pp. 922–923, 1988.

[8] G. Joyce, V. Lanzisera, and R. Olshansky, "Improved sensitivity of 60 video channel FM-SCM receiver with semiconductor optical amplifier," *Electron. Lett.*, vol. 25, pp. 499–501, 1989.

[9] J. Stern, J. Ballance, D. Faulkner, S. Hornung, and D. Payne, "Passive optical local networks for telephony applications and beyond," *Electron. Lett.*, vol. 23, pp. 1255–1256, 1987.

[10] R. Olshansky and V. Lanzisera, "Subcarrier passive optical network for low cost video distribution," in *Proc. Opt. Fibre Commun. Conf.*, 1989, p. 57.

[11] J. Gimlett, "A new low noise 16 GHz PIN/HEMT optical receiver," in *Proc. European Conf. Opt. Commun.*, 1988, pp. 13–16.

[12] G. Jacobsen, J. Kan, and I. Garrett, "Tuned front-end design for heterodyne optical receivers," *J. Lightwave Technol.*, vol. 7, pp. 105–114, 1989.

[13] J. Kan, I. Garrett, and G. Jacobsen, "Transformer tuned front ends for heterodyne optical receivers," *Electron. Lett.*, vol. 23, pp. 785–786, 1987.

[14] T. Darcie, B. Kasper, J. Talman, and C. Burrus, "Resonant pin-FET receivers for lightwave subcarrier systems," *J. Lightwave Technol.*, vol. 6, pp. 582–589, 1988.

[15] A. Cappy, "Noise modeling and measurement techniques," *IEEE Trans. Microwave Theory Tech.*, vol. 36, pp. 1–10, 1988.

[16] R. Minasian, "Optimum design of a 4-Gbit/s GaAs MESFET optical preamplifier," *J. Lightwave Technol.*, vol. LT-5, pp. 373–379, 1987.

[17] K. Ogawa, "Noise caused by GaAs MESFETs in optical receivers," *Bell Syst. Tech. J.*, vol. 60, pp. 923–928, 1981.

[18] K. Tanaka *et al.*, "Low-noise HEMT using MOCVD," *IEEE Trans. Electron. Devices*, vol. ED-33, pp. 2053–2058, 1986.

[19] R. Olshansky and V. Lanzisera, "60 channel FM video subcarrier multiplexed optical communication system," *Electron. Lett.*, vol. 23, pp. 1196–1197, 1987.

[20] M. Abuelma'atti, "Carrier-to-intermodulation performance of multiple FM/FDM carriers through a GaAlAs heterojunction laser diode," *IEEE Trans. Commun.*, vol. COM-23, pp. 246–248, 1985.

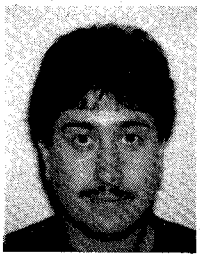

Kamal E. Alameh (S'89) received the B.Eng. Sc. degree from Beirut Arab University, Beirut, Lebanon, in 1985, and M.Eng.Sc. degree from the University of Melbourne, Melbourne, Australia, in 1989. He is currently pursuing the Ph.D. degree in electrical engineering at the University of Sydney, Sydney, Australia.

He has done work in the area of digital filter analysis, design, and simulation, as well as in the performance analysis and design of coherent and direct-detection optical receivers. His current interests include the analysis, design, and simulation of tuned optical receivers for microwave subcarrier multiplexed lightwave systems. In addition, he is also currently interested in the simulation of nonlinear distortion of multiple FM/FDM carriers through laser diodes.

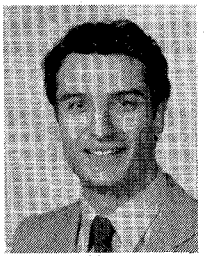

Robert A. Minasian (S'78–M'80) was born in May 1953. He received the B.E. (elec.) degree from the University of Melbourne, Australia, and the M.Sc. degree (with distinction) from University College, University of London, in 1976. He was awarded the Ph.D. degree from the University of Melbourne in 1980.

During the year 1983 he was a Visiting Research Fellow at the Laboratoires d'Electronique et de Physique Appliquée, France, and in 1988 he was with the GEC Hirst Research Centre, England, where he was engaged in research on high-speed lightwave systems. Prior to 1989 he was at the University of Melbourne. He is presently an Associate Professor in Electrical Engineering at the University of Sydney, Australia. His current research interests include high-data-rate lightwave systems, microwave and optoelectronic devices, and high-speed integrated circuits for microwave and fibre-optic communications.

Dr. Minasian is a senior member of the IREE.